

# A GEODETIC REFERENCE FRAME FOR THE VIRGO INTERFEROMETER

A. Paoli, EGO - European Gravitational Observatory, Pisa, Italy  
M. Marsella, C. Nardinocchi, DICEA-Survey Lab, Università di Roma “La Sapienza”, Italy  
L. Vittuari, A. Zanutta, DICAM, Università di Bologna, Italy

## Abstract

The Virgo detector, currently in its 2<sup>nd</sup> generation configuration Advanced Virgo (AdV), is a Michelson interferometer aimed at the gravitational waves research and at opening a new window on the study of the Universe. It is made of two orthogonal arms being each 3 kilometers long and is located at the site of the European Gravitational Observatory (EGO), in the countryside near Pisa, Italy (Figure 1).

This paper reports the development of the Virgo Reference System (VRS) that since 2012 was established for the installation of Advanced Virgo [1]. The VRS consists of a wide-scale high precision reference network adopted for the alignment of new equipments and for the displacement of the existing ones. This reference will be adopted for periodic checks and monitoring activity.

Considering the weakness of the network geometry, the survey activity was conducted integrating classical and GNSS measurements by applying the necessary corrections to reduce the coordinates into a unique reference system. Tridimensional coordinates were derived from the GNSS observations and merged with the total station (TS) observations, after applying the appropriate corrections. In addition, a rigorous method to define the relation between orthometric and topographic heights, needed for both design/construction and alignment activities, was carried out.



Figure 1: Aerial view of Virgo Site.

## INTRODUCTION

The main purpose of the work is the establishment of a wide-scale high precision reference network to define the Virgo Reference System (VRS). The activity was carried out simultaneously with the construction of Advanced Virgo, upgraded configuration of the Virgo detector which operated between 2004 and 2011. AdV is designed to

improve the sensitivity by a factor 10 better than Virgo, thus allowing the observation of a volume of the Universe 1000 times larger.

The availability of a high precision reference system is fundamental to carry out all the surveying activities, needed in a research facility that hosts large experimental apparatus such as Virgo [2], [3], [4], [5] and [6]. Similarly to other research facility sites, many geodetic activities are required at Virgo:

- alignment of the new equipment installed for AdV or displacement of the existing ones;
- determination of the position of the internal components of the detector (mirrors, payloads, super-attenuators, in-air benches, suspended benches, etc.) in the VRS as the unique reference system;
- execution of periodic checks;
- monitoring over time of the (relative) position for the several buildings hosting the scientific apparatus.

The VRS was established by of a number of new reference points, which integrated and enlarged the previous local networks. Through GNSS measurements, a cross-connection between the two Virgo tunnels was obtained in order to increase the robustness of the network configuration, improving the reliability of the final VRS coordinates [7]. Additional links with the secondary networks placed in the experimental building (Central Building, Mode Cleaner, West End Building and North End Building) were performed in order to obtain in all sections of the Virgo facility a set of congruent coordinates.

Therefore the estimated solution for the network coordinates includes both the new points defined for the establishment of VRS and the ones selected to tie it to the existing old local networks.

This paper describes the surveying activities that have been carried out and contains a summary of the processing strategy adopted to perform the network adjustment and obtain the final set of coordinates of the VRS network.

## ESTABLISHMENT OF THE VIRGO REFERENCE SYSTEM

The reference frame for the VRS solution was defined by fixing the alignment between two points GPS00N-GPS10N (Table 1) established using a device designed by EGO during previous GPS surveys to guarantee a precise antenna positioning for the monitoring of the horizontal displacements of the tunnels. Therefore, the direction of the Y-axis is parallel to the North Arm and the X-axis accordingly perpendicular to the Y-axis.

Table 1: 2D Coordinates of the points used to define the orientation of the reference frame

Point ID	x (m)	y (m)
GPS00N	2.5044	97.9756
GPS10N	2.5075	2918.0138

### ACTIVITY DESCRIPTION

The conducted activity included three main phases, the design of the network, the collection of the measurements and the data processing, hereafter described.

#### Network Design

In order to identify a number of possible free sight-line connections to be adopted for a preliminary design of the network configuration, an on-site inspection was carried out.

As mentioned above, in consideration of the dimension of the network and the necessity to link the external network with the internal one, it was decided to integrate TS measurements with GNSS baselines.

This integrated approach not only increased the robustness of the network but also allowed to established links between the terminal parts of the two tunnels, not mutually measurable with optical instruments.

The TS measurements were performed starting from existing references mounted on 4 concrete pillars, located in the external area close to the Central Building, previously connected with the network inside the building. Additional points were positioned along the arms and on the bridges passing over the tunnels. This allowed to perform optical measurements linking the Central Building with the North and West End Buildings.

The final VRS network configuration is reported in Figure 2, showing both the external network and the main reference points inside the buildings.

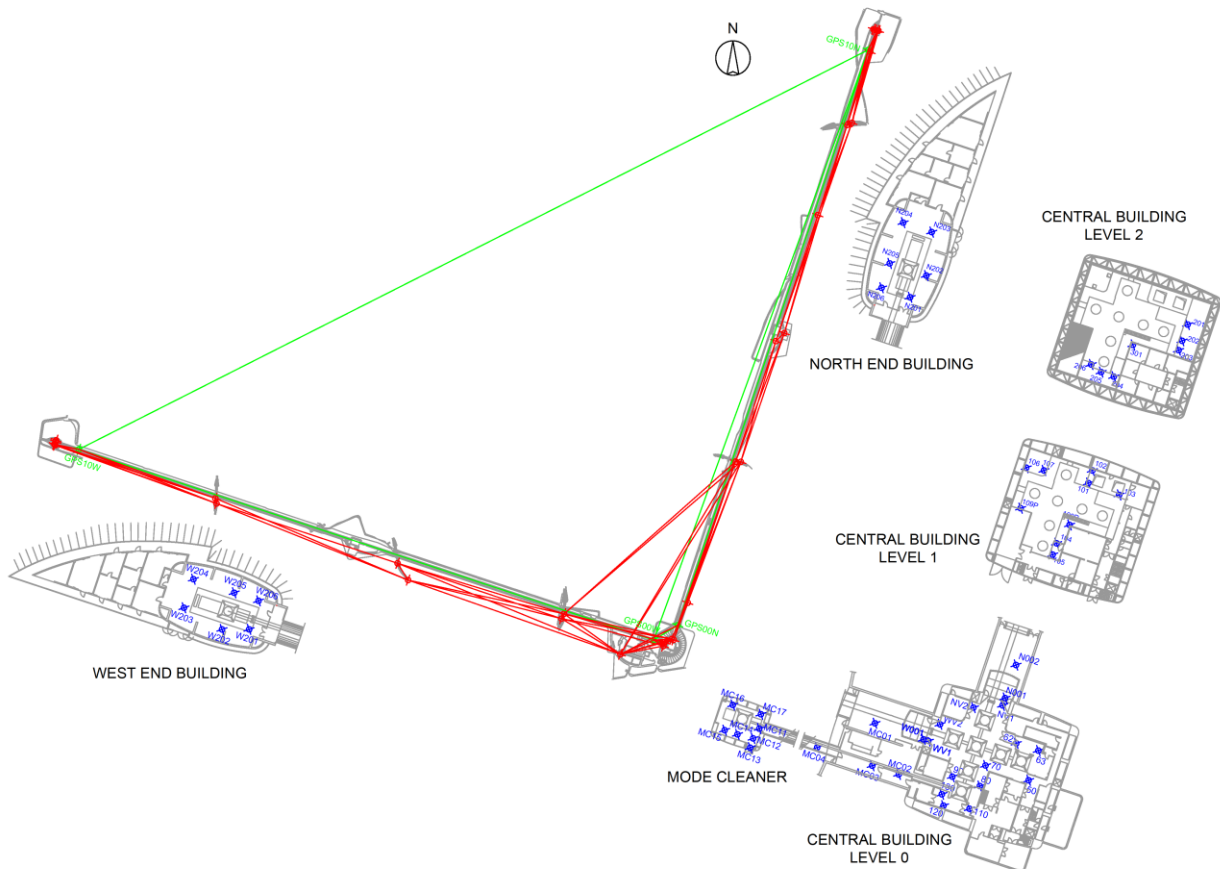


Figure 2: Complete layout of the VRS surveyed network (two orthogonal arm each 3 km long): green lines show the GNSS network and red lines the external TS network, distributed along the arms; blue points shows the (main) VRS internal reference point network, located inside the four experimental buildings.

## Network Measurement

Two Total Station campaigns (18÷19 June and 15÷16 July 2014) were performed using a Leica TM50 and a Leica TDA5000 instruments. Additional measurements, using a Leica TDA 5000, were performed on 2 September and on 22 October 2014. The first two campaigns allowed linking the 4 external pillars to the external part of the North and West End Buildings; the third and the fourth ones allowed to connect the external surveys with the reference points located in the experimental buildings.

The observations of slope distance, azimuthal and vertical angle were repeated three times, in both forward and backward mode, and then averaged to obtain a set of measurements for each surveyed point. The TS observations were acquired in a fully automated mode, achieving a better precision.

The technical specifications of the TS instruments are listed in Table 2.

Table 2: Technical specification of the TS instruments

		TM50	TDA5000
Angle measurement accuracy	Azimuth	0.5"	0.15 mgon
	Zenith	1"	0.3 mgon
Distance measurement with prism	Max distance	3500 m	2500 m
	Accuracy	0.6mm+1ppm	1mm+2ppm

The GNSS survey was performed on 11÷13 July 2014 (JD 192÷194) using five geodetic receivers (four Trimble 5700 and one Topcon GB100), all of them connected to Choke Ring antennas. The acquisitions were composed by 24 hours lasting sessions (Figure 3). Each session was processed separately using the Bernese scientific software v.5.0 to obtain a network solution including 10 GNSS stations of the EUREF Permanent Network linked to the ETRF reference frame.



Figure 3: GNSS antenna mounted on the tunnel.

The solutions of the three sessions were averaged both for the coordinates and for the corresponding errors, obtaining the results summarized in Table 3.

Table 3: Solution of the GNSS processing

Point ID	X (m)	Y (m)	Z (m)
GPS00N	4546307.124	843013.321	4378645.366
GPS10N	4544331.414	843601.216	4380569.835
GPS00W	4546373.099	842910.486	4378597.265
GPS10W	4546219.966	840177.392	4379274.960

Point ID	$\sigma_x$ (m)	$\sigma_y$ (m)	$\sigma_z$ (m)
GPS00N	0.001	0.001	0.001
GPS10N	0.001	0.001	0.001
GPS00W	0.001	0.001	0.001
GPS10W	0.001	0.001	0.001

## Data Processing

GNSS coordinates were transformed from the 3D Cartesian geocentric reference system (ETRF00) in a Eulerian Reference System (ERS) with the origin posed in the Central Building and y axis along the North direction (Figure 4), and the baseline calculated respect this Cartesian local reference system

Before integrating with the GNSS baselines, the TS raw observations (azimuth, zenith and slope distance for each point) were corrected to take into account the terrestrial curvature and transform them in the same tridimensional Cartesian system. As a matter of fact, due to the extension of the surveyed network, which spreads over an area of about 550.000 m<sup>2</sup> along the two arms, the simplifications usually adopted (i.e. gravitational field perpendicular to a local plane) could not be considered.

## Terrestrial curvature and atmospheric corrections of the total station raw observations

Slope distance values were corrected for the refraction effect according to Eq. 1:

$$\Delta D = 286.34 - \left[ \frac{0.29525 \cdot p}{1 - \alpha \cdot t} - \frac{4.126 \cdot 10^{-4} \cdot h}{1 - \alpha \cdot t} \cdot 10^x \right] \quad (1)$$

$\Delta D$  = atmospheric correction (ppm)

$p$  = air pressure (mbar)

$t$  = air temperature (°C)

$h$  = relative humidity (%)

$\alpha = 1/273.15$

$x = 7.5 \cdot t / (237.3 + t) + 0.7857$

where the average atmospheric parameters (air temperature, pressure and relative humidity) used in the formula were provided by the local EGO meteo-station.

Azimuthal, zenithal and distance measurements were corrected in order to refer them to the tridimensional Cartesian reference system (ERS) according to the formulas given in [8]. These corrections take into consideration the variation of the angle between the vertical axis (z-axis) of the ERS reference system and the normal to the local sphere having the average radius of curvature in the surveyed area, respect to which the observations acquired by the TS are referred.

### Transformation of GNSS ETRF coordinates in ERS

The coordinates of the points GPS00N, GPS10N, GPS00W and GPS10W, obtained by the Bernese network solution, were transformed in the ERS reference frame.

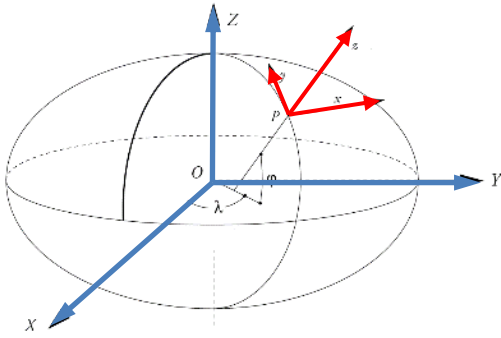


Figure 4: ETRF and ERS reference systems.

An approximate position for the origin of the ERS was selected in correspondence of the Central Building (Table 4). Its geographic coordinates ( $\phi_0$ ,  $\lambda_0$ ) provide the angles for the rotation matrix between ETRF and ERS, while the 3D ETRF coordinates of the origin ( $X_0$ ,  $Y_0$ ,  $Z_0$ ) represent the translation parameters.

Table 4: Coordinates of the approximate origin

	$\phi_0$	$\lambda_0$	$H_0$ (m)
Origin	10° 30' 16".12	43° 37' 53".10	9.0

Point ID	$X_0$ (m)	$Y_0$ (m)	$Z_0$ (m)
Origin	4546337.287	842981.326	4378541.338

In Table 5 the ERS coordinates, with corresponding rms, of the four GPS point obtained following the analytical transformation  $\mathbf{x}_{ERS} = \mathbf{R}(\phi_0, \lambda_0) \cdot (\mathbf{X} - \mathbf{X}_0)$  are shown.

Table 5: GPS point coordinates in the ERS frame

Point ID	x (m)	y (m)	z (m)
GPS00N	36.9591	91.7334	51.5944

GPS10N	975.1959	2751.1191	50.7633
GPS00W	-76.1818	25.0953	51.5020
GPS10W	-2735.5504	963.3168	49.4951

Point ID	$\sigma_x$ (m)	$\sigma_y$ (m)	$\sigma_z$ (m)
GPS00N	0.0002	0.0003	0.0011
GPS10N	0.0002	0.0002	0.0080
GPS00W	0.0002	0.0003	0.0011
GPS10W	0.0002	0.0003	0.0011

## OBSERVATION ADJUSTMENT

The network adjustment, based on a least square method and performed with the scientific software CALGE (Forlani, 1986) [9], was aimed at determining the best estimate of the coordinates of the established set of points with their relative (intrinsic/internal) accuracy.

The software requires as input the total station observations that are used to form a redundant set of observation equations for each 3D range, azimuthal and zenithal observations, and the baseline component. The error model used in the adjustment (rms associated to each observations) was defined accordingly to the instrument specifications.

Therefore the adjustment was performed in the ERS.

### Outlier detection of TS data

A first preliminary network adjustment of the TS observation was performed in order to check the TS measurements before the integration with GNSS data. The solution was computed in the ERS reference frame established by the four GPS points.

### Combined TS and GNSS Network adjustment data

Final network adjustment was performed using both TS and GNSS measurements. The following GNSS baselines were used to constrain the network (Table 6) using the associated rms:

Table 6: GNSS baselines used in the network adjustment

Baseline	$\Delta x$ (m)	$\Delta y$ (m)	$\Delta z$ (m)
GPS00N-GPS00W	-113.1409	-66.6381	-0.0924
GPS00N-GPS10W	-2772.5095	871.5834	-2.0993
GPS00N-GPS10N	938.2368	2659.3858	-0.8311
GPS00W-GPS10W	-2659.3685	938.2215	-2.0069
GPS00W-GPS10N	1051.3777	2726.0239	-0.7387
GPS10N-GPS10W	-3710.7462	-1787.8023	-1.2682

Baseline	$\sigma_{\Delta x}$ (m)	$\sigma_{\Delta y}$ (m)	$\sigma_{\Delta z}$ (m)
GPS00N-GPS00W	0.0010	0.0010	0.0020
GPS00N-GPS10W	0.0010	0.0010	0.0020
GPS00N-GPS10N	0.0010	0.0010	0.0020
GPS00W-GPS10W	0.0010	0.0010	0.0020
GPS00W-GPS10N	0.0010	0.0010	0.0020
GPS10N-GPS10W	0.0010	0.0010	0.0020

Considering the wide range of lengths between the surveyed points, the error model for the TS observations was defined as a function of the distance. Several tests were performed to verify if the adopted model provided results in agreement with the assigned accuracy. Finally, on the basis of the conducted tests, previous experiences and literature data, the rms indicated in Table 7 and 8 were adopted.

Table 7: rms of slope distance of the used TS

D (m)	TM50		TDA5000	
	$\sigma$ (mm)	ppm	$\sigma$ (mm)	ppm
< 200	0.6	1	1	2
$\geq$ 200	1	1	1.5	2

Table 8: angular rms used in the network adjustment

D (m)	TM50		TDA5000	
	$\sigma_H$ (cc)	$\sigma_V$ (cc)	$\sigma_H$ (cc)	$\sigma_V$ (cc)
< 5	20	30	20	30
5-10	15	25	15	25
10-50	10	20	10	20
50-200	8	15	8	15
> 200	5	10	5	10

### Transformation from ERS to VRS reference frame

The adjusted network was rotated to match the alignment between the baseline initially considered GPS00N-GPS10N (Table 1) and the GPS00N-GPS10N calculated in the ERS reference system. The rotation angle is equal to  $-0.011472$  gon.

Successively, in order to set the VRS origin coincident with that of the old reference system, the translation along x and y axis of the network was calculated. To determine the shift parameters, the network was integrated, and adjusted, with the observation surveyed on 22 October 2014, which contain a set of five reference points known in the old reference system. The transformation parameters were calculated with a least square method on a set of those five reference points.

### Height correction

Point heights were corrected by shifting the whole network in the Z direction of a value calculated as the average of the differences between the heights of six reference points, belonging to the Central Building, and the corresponding heights determined by previous surveys.

## RESULTS

The following Table 9 reports the Max e min rms associated to the final coordinates, for both the VRS network points (i.e. the monumented points placed inside the buildings and used for the subsequent alignments and monitoring activities) and the whole network.

Table 9: Max e min rms values

		$\sigma_x$ (mm)	$\sigma_y$ (mm)	$\sigma_z$ (mm)
VRS	Max	1.2	1.3	1.8
	min	0.1	0.1	0.3
whole network	Max	3.0	2.5	4.0
	min	0.1	0.1	0.1

## GEOGRAPHIC LOCATION OF VIRGO

The establishment of the VRS reference frame and the determination of the transformation parameters between ETRF and VRS have also allowed the inverse transformation VRS  $\rightarrow$  ETRF and the estimation of the ETRF coordinates of the ‘‘Virgo Vertexes’’, i.e. the centers of the Beam Splitter, North End and West End suspended mirrors (Table 10, 11 and 12). Indeed, the VRS coordinates of the mirrors centers (not visible with a direct survey), have been calculated by the optical characterization of the interferometer in VRS coordinates and used for the alignment of the mechanical suspension of the mirrors (Figure 5).

Table 10: VRS coordinates of the Virgo vertexes

Point ID	X (m)	Y (m)	Z (m)
BS	0.0027	0.0232	-0.0030
NE	0.0129	3005.7877	-0.9020
WE	-3005.5847	0.0312	-2.2233

Table 11: ETRF coordinates of the Virgo vertexes

Point ID	X (m)	Y (m)	Z (m)
BS	4546374.575	842990.280	4378578.106
NE	4544268.524	843616.857	4380629.099
WE	4546211.299	840077.332	4379300.349



Table 12: ETRF geographic coordinates of the Virgo vertexes

Point ID	LAT	LONG	h (m)
BS	43° 37' 53".1061 N	10° 30' 16".2095 E	53.089
NE	43° 39' 24".9464 N	10° 31' 00".8387 E	52.899
WE	43° 38' 25".4873 N	10° 28' 09".7533 E	51.575

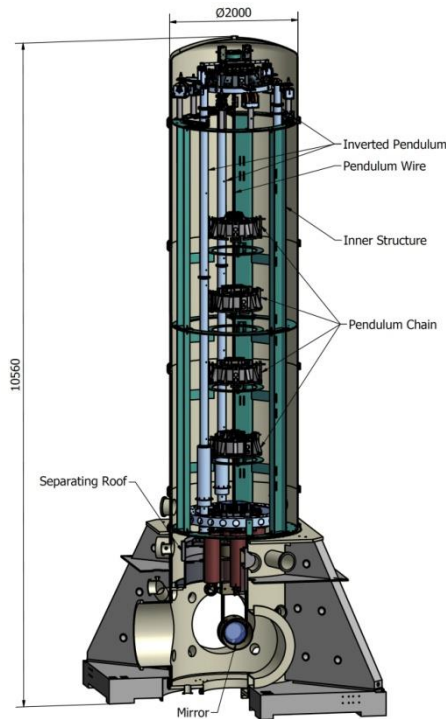


Figure 5: Virgo tower isometric view: 11 m high vacuum chamber with the mechanical suspension chain and the suspended mirror.

Besides, the ETRF coordinates allowed also to determine the global alignment of the local network respect to the geographic North.

The azimuth of the geodetic curve through BS and NE, with respect to the geographic North, is:

$$19.43297959^\circ = 19^\circ 25' 58''.7265$$

The azimuth of the geodetic curve through BS and WE, with respect to the geographic North, is:

$$289.43293666^\circ = 289^\circ 25' 58''.5720.$$

The geographic location and the orientation of Virgo respect to the other Gravitational Waves (GW) detectors (LIGO Hanford, WA, USA; LIGO Livingston, LA, USA; GEO, Germany; TAMA, Japan) are fundamental for the contemporary detection of signals coming from the Universe, which will start the era of the GW Astronomy.

## CONCLUSION

Installation and management of a complex research infrastructure such as Virgo, requires a series of high-precision geodetic surveying activities for the mutual positioning of the various instrumental parts and, at the same time, for the monitoring of the movements (especially vertical) elapsing in time among the different parts of the interferometer.

Both terrestrial and space geodesy measuring instruments were used in this work: high precision total stations and geodetic GNSS receivers. The main advantage from the integration of the two techniques is the enforcement of the robustness of the geodetic reference network. In particular the use of GNSS allowed the link between the terminal parts of the two tunnels of the interferometer, not mutually measurable with optical instruments.

A further relevant aspect of the work has been the determination of the accurate geographic position of Virgo respect to the other interferometers of the GW detector network which is, in fact, fundamental for the contemporary detection of signals coming from the Universe, which will start the era of the GW Astronomy.

The accuracy obtained for both the VRS network points coordinates and the transformation parameters between the different reference systems, have been in line with the initial specifications, considering the used instruments and the adopted surveying methodologies.

## REFERENCES

- [1] The Virgo Collaboration, "Advanced Virgo Technical Design Report", VIR-0128-12, EGO TDS, April 2012.
- [2] D. Missiaen, T. Dobers, M. Jones, C. Podevin, J.P. Quesnel, "The final alignment of the LHC". IWAA08, Tsukuba, February 2008.
- [3] D. Missiaen, P. Dewitte, J.-F. Fuchs, H. Mainaud Durand, T. Dobers, M. Jones, J.-C. Gayde, "Status report of projects activities at CERN". IWAA14, IHEP, Beijing, October 2014.
- [4] C. Le Cocq, R. Ruland, "Status Report on Alignment Activities at SLAC". IWAA08, Tsukuba, February 2008.
- [5] B. O'Sheg Oshinowo, H. Friedsam, "Survey of the NOvA Near Detector at Fermilab". IWAA10, DESY Hamburg, September 2010.
- [6] R. Beunard, A. Lefevre, F. Legruel, "The Initial Geodetic Survey for the SPIRAL2 Process Installation". IWAA10, DESY Hamburg, September 2010.
- [7] S. Matsui, H. Kimura, RIKEN, Kouto, Sayo-cho, Sayo-gun, Hyogo "Survey Comparison using GNSS and ME5000 for One kilometer Range". IWAA08, Tsukuba, February 2008.
- [8] M. Brovelli, F. Sansò, "Equazioni di osservazione della topografia in coordinate cartesiane locali: scrittura, linearizzazione e analisi dei relativi ambiti di validità". – Anno XLVIII, Bollettino di Geodesia e Scienze affini n.3, 1989.
- [9] G. Forlani, "Sperimentazione del nuovo programma CALGE dell'ITM." Bollettino SIFET, n.2, 1986.

## ATTACHED DOCUMENT

*Table of coordinates of the VRS reference frame and their associated rms.*

Point ID	X (m)	Y (m)	Z (m)
70	3.4185	-3.5306	-1.0683
80	3.6523	-8.4941	-1.0736
100	-47.6449	-1.0279	0.0421
150	0.9390	46.8017	0.0901
200	-22.7279	0.7896	4.3028
300	-53.8469	-7.0541	-0.0562
301	5.1781	-5.1678	9.2305
500	2.9616	2997.5477	-0.8246
1001	-516.7152	-18.0099	3.3605
1002	-208.7804	-114.2484	6.6215
1003	18.7070	905.3844	3.0144
1004	42.3085	912.0774	0.2176
1005	20.4295	1496.4293	-2.3512
1006	46.1996	1544.4685	-3.2842
1007	21.4751	2114.5778	-1.3471
1008	19.2846	2555.4140	2.9135
1009	37.3214	2572.4841	1.6719
1010	20.1311	3017.9991	-2.4721
1011	13.5255	3016.1793	-2.3278
2001	-521.0425	-43.2501	2.1521
2002	-1255.2989	-97.5482	-3.7849
2003	-1326.6115	-38.7055	-0.3579
2004	-2214.3196	-39.9086	-1.1410
2005	-2227.3858	-18.6097	1.6533
2006	-3012.4814	-18.9375	-4.0081
2007	-3017.9492	-15.6923	-4.0425
108P	4.3951	-4.4076	3.5298
C6	5.8391	27.8516	3.7404
C7	-4.0877	27.7952	3.7171
C8	-29.7819	3.9608	3.6936
C9	-30.0540	-14.4490	3.5099
GPS00N	2.5067	97.9809	-1.4923
GPS00W	-82.0171	-2.5013	-1.5897
GPS10N	2.5098	2918.0193	-2.3266
GPS10W	-2902.0355	-2.5090	-3.5945
MC01	-24.1098	-2.3039	-1.0763
MC03	-21.6066	-11.8615	-1.0869
N001	2.8007	12.8086	-1.0610
N002	2.8048	20.8946	-1.0773
N004	2.5014	50.8881	-1.4704
N201	2.5123	3000.4417	-1.9587
N202	4.5122	3006.4208	-1.9944
N203	2.5121	3016.4159	-1.9960
N204	-4.4880	3016.4142	-2.0013
N205	-4.4912	3006.4167	-1.9903
N206	-4.4928	3000.4447	-1.9849
NV1	2.8020	11.0011	-1.0722
NV2	-3.4744	8.3776	-1.0696
P12N	13.8827	2911.8992	-1.3676
P1N	13.9143	211.9612	-0.1808
W001	-12.2065	-2.3015	-1.0680
W004	-50.0811	-2.5058	-1.5296
W201	-2999.5794	-2.4737	-3.2731
W203	-3015.5745	-2.4752	-3.4065
W204	-3015.5788	4.5200	-3.4158
W205	-3005.5809	4.5203	-3.3696
W206	-2999.5839	4.5218	-3.3487
WE1	-3004.4334	1.0324	-0.5980
WE3	-3006.5849	1.1805	-0.6004
WE4	-3006.7353	1.0298	-0.6004
WE5	-3006.7351	-0.9692	-0.6000
WE6	-3006.5845	-1.1198	-0.5996
WE7	-3004.5840	-1.1187	-0.5962
WE8	-3004.4329	-0.9683	-0.5976
WV1	-10.9996	-2.3030	-1.0711

Point ID	$\sigma_x$ (mm)	$\sigma_y$ (mm)	$\sigma_z$ (mm)
70	0.80	0.60	0.72
80	0.90	0.70	0.80
100	0.30	0.30	0.34
150	0.50	0.40	0.55
200	0.20	0.20	0.26
300	0.30	0.20	0.34
301	0.80	1.00	0.99
500	1.00	0.70	1.32
1001	0.50	1.20	1.45
1002	0.40	0.70	0.84
1003	2.20	1.00	4.03
1004	2.20	1.00	4.03
1005	3.00	1.20	3.68
1006	3.00	1.30	3.67
1007	2.70	1.20	3.25
1008	1.70	0.80	1.78
1009	1.60	0.70	1.75
1010	0.90	0.70	1.31
1011	1.00	0.70	1.31
2001	0.60	1.30	1.50
2002	0.90	2.50	4.03
2003	1.00	2.50	4.05
2004	1.00	2.20	3.14
2005	1.00	2.20	3.14
2006	0.70	1.10	1.67
2007	0.70	1.10	1.67
108P	0.80	1.10	0.85
C6	0.10	0.10	0.09
C7	0.20	0.10	0.19
C8	0.20	0.20	0.24
C9	0.30	0.20	0.28
GPS00N	0.30	0.30	0.42
GPS00W	0.10	0.10	0.09
GPS10N	0.60	0.50	1.17
GPS10W	0.50	0.60	1.17
MC01	0.50	0.50	0.46
MC03	1.00	0.60	0.65
N001	0.70	0.50	0.65
N002	0.60	0.60	0.62

N004	0.50	0.40	0.55
N201	1.00	0.90	1.36
N202	1.00	0.80	1.33
N203	1.00	0.60	1.31
N204	1.00	0.70	1.31
N205	1.00	0.80	1.33
N206	1.00	0.70	1.33
NV1	0.70	0.50	0.59
NV2	1.20	0.50	0.70
P12N	0.70	0.60	1.21
P1N	1.10	0.70	1.11
W001	0.40	0.50	0.39
W004	0.30	0.30	0.34
W201	0.90	1.10	1.75
W203	0.70	1.20	1.68
W204	0.80	1.10	1.68
W205	1.20	1.20	1.73
W206	1.20	1.30	1.79
WE1	1.10	1.30	1.74
WE3	0.90	1.10	1.70
WE4	1.20	1.20	1.73
WE5	0.90	1.20	1.70
WE6	0.90	1.20	1.70
WE7	1.20	1.20	1.73
WE8	1.20	1.20	1.73
WV1	0.50	0.50	0.55